SCIENTIFIC REPORTS

SUBJECT AREAS:
BIOPHYSICS
CELL SIGNALLING
DISEASES
CHANNELS

Received
31 January 2012

Accepted
22 March 2012

Published
17 April 2012

Correspondence and requests for materials should be addressed to D.A. (datlas@vms.huji.ac.il)

* Equal contribution.

Calcineurin Controls Voltage-Dependent-Inactivation (VDI) of the Normal and Timothy Cardiac Channels

Moshe Cohen-Kutner*, Yfat Yahalom*, Michael Trus & Daphne Atlas

The Hebrew University of Jerusalem Institute of Life Sciences Dept. of Biological Chemistry Givat-Ram, Jerusalem, 91904, Israel.

Ca^{2+}-entry in the heart is tightly controlled by Cav1.2 inactivation, which involves Ca^{2+}-dependent inactivation (CDI) and voltage-dependent inactivation (VDI) components. Timothy syndrome, a subtype-form of congenital long-QT syndrome, results from a nearly complete elimination of VDI by the G406R mutation in the $\alpha_1$1.2 subunit of Cav1.2. Here, we show that a single (A1929P) or a double mutation (H1926A-H1927A) within the CaN-binding site at the human C-terminal tail of $\alpha_1$1.2, accelerate the inactivation rate and enhances VDI of both wt and Timothy channels. These results identify the CaN-binding site as the long-sought VDI-regulatory motif of the cardiac channel. The substantial increase in VDI and the accelerated inactivation caused by the selective inhibitors of CaN, cyclosporine A and FK-506, which act at the same CaN-binding site, further support this conclusion. A reversal of enhanced-sympathetic tone by VDI-enhancing CaN inhibitors could be beneficial for improving Timothy syndrome complications such as long-QT and autism.

The inactivation of the L-type voltage-gated calcium channel Cav1.2 plays a central role in controlling excitation-contraction (E–C) coupling in cardiac myocytes and consists of two independent mechanisms, CDI and VDI (for reviews, see[1–6]).

Early studies revealed CDI signaling to be predominantly mediated by Ca^{2+}/calmodulin binding to an IQ motif at the proximal C-tail of the $\alpha_1$1.2 subunit of Cav1.2[7–11]. A proteolytically cleaved distal domain has been suggested to form a non-covalent complex with the proximal C-tail acting like an autoinhibitory motif[12]. While CDI has been extensively studied and is well documented, the exact mechanism by which VDI regulates Cav1.2 remains largely unknown. The importance of VDI became apparent by the discovery of a mis-sense mutation G406R at the $\alpha_1$1.2 pore forming subunit of Cav1.2 that manifests itself in the Timothy syndrome (TS). In TS, VDI impairment resulted in prolonged QT interval, and severe arrhythmias in the heart, accompanied by an autism spectrum disorder[13,14].

The well documented participation of calcineurin (CaN), a Ca^{2+}/calmodulin-dependent protein IIB phosphatase, in controlling Ca^{2+} signaling in mouse ventricular myocytes[15–20], has prompted a search for CaN binding site(s) within the $\alpha_1$1.2 subunit.

Previous in vitro binding experiments have demonstrated that CaN binds to the C-tail of rabbit $\alpha_1$1.2 at a minimal site spanning amino acids D1943-L1971[21], and to undefined sites downstream of L1971[22]. Deletion of large segments comprising 285, 405 or 438 amino acids at the C-terminus, which comprise of the CaN-binding site, increased channel activity[23], are consistent with the elimination of a VDI regulatory interface at the rabbit $\alpha_1$1.2 C-terminus[24,25,12].

Here we have combined molecular, electrophysiological, and pharmacological approaches to establish CaN as a VDI-regulatory protein of the human Cav1.2 channel. Although CaN binding site at the C-tail of $\alpha_1$1.2 was established[21,22], the functional effect of CaN on Cav1.2 properties is not known. We show that a single point mutation A1929P at CaN binding motif accelerates Cav1.2 inactivation and increases the extent of VDI. The A1929P mutation, previously shown to abrogate binding of CaN to the channel[21,22], accelerated channel inactivation most likely by preventing CaN binding to the CaN-binding motif within the C-tail of the channel. The mutation also restored the impaired voltage inactivation of the Timothy G406R-channel. These results identify the CaN binding motif as a negative modulator of VDI. VDI restoration by CaN selective inhibitors cyclosporine

A and FK506 confirm CaN as a regulator of VDI, and implicate the CaN-binding site in the $\alpha_1$1.2 subunit as a potential therapeutic target for TS and other arrhythmias.

Results

Mutations within the CaN binding motif, A1929P, or H1926A/H1927A, accelerate the rate of Cav1.2 voltage-dependent inactivation. The most distal C-terminal domain of rabbit $\alpha_1$1.2 comprises a putative CaN minimal binding motif D1943-L1971[21], corresponding to D1913-L1941 of the human $\alpha_1$1.2 subunit (**Fig. 1a, *upper***), a phosphatase 2A (PP2A)-binding site at L1935−R1941, and an additional CaN binding-site downstream of R1941[22]. Both CaN and PP2A sites are located downstream to the PKA interaction domain[26–28].

The functional impact of the CaN binding motif on Ca_V1.2 properties was tested in BAPTA-injected *Xenopus* oocytes, using the two-electrode-voltage-clamped assay. Both CaN[29] and cyclophilin[30] are natively expressed in *Xenopus* oocytes.

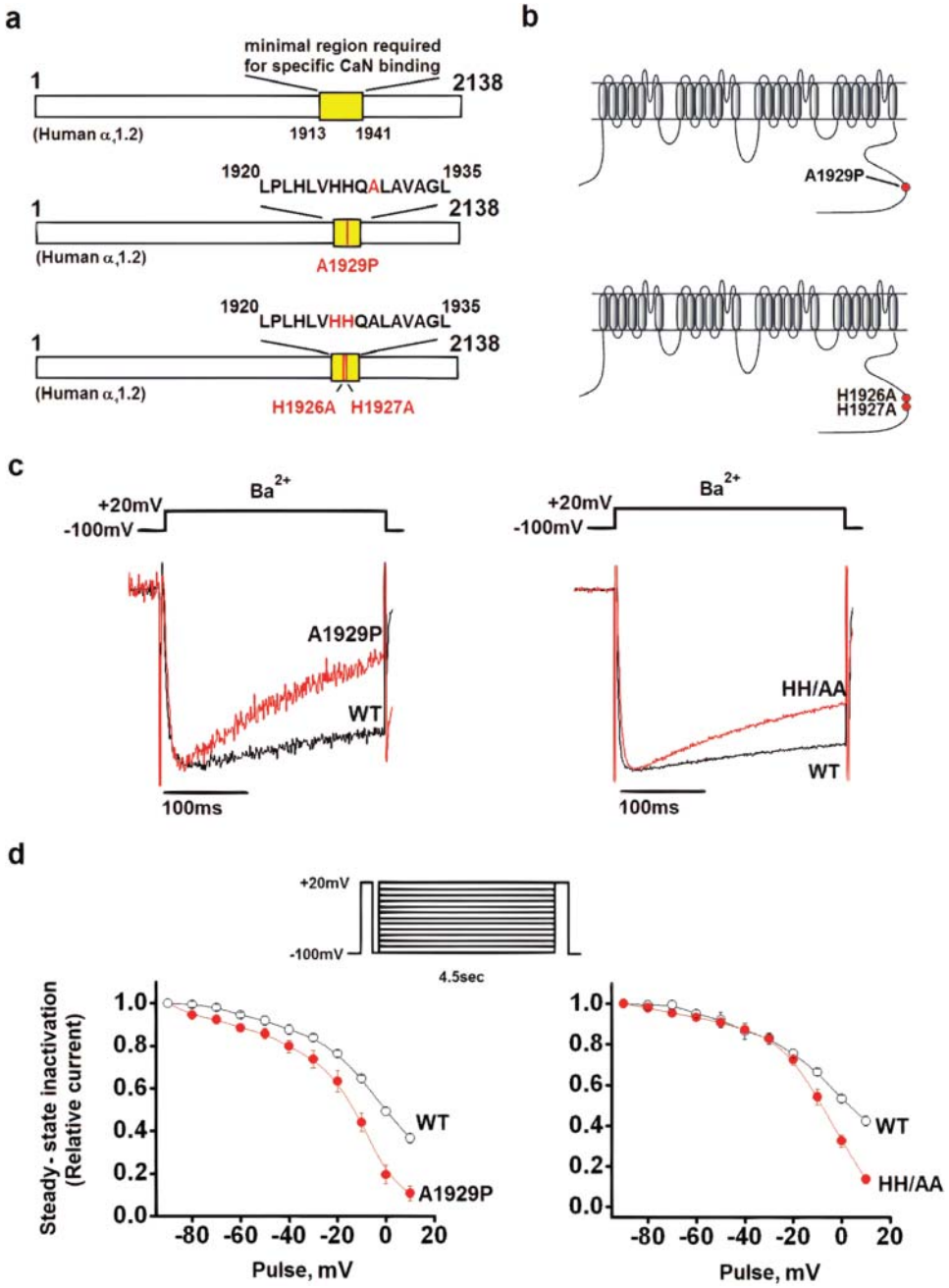

Figure 1 | Single and double amino acid mutations within the CaN binding motif at the C-tail of $\alpha_1$1.2 subunit restore VDI of Cav1.2. (Ba) Schematic presentation of: the minimal CaN-binding site (*upper*), Ala 1929 (*middle*) and His1926, His1927 residues within this minimal CaN- binding domain (*lower*). (b), Schematic illustration of channel mutants: $\alpha_1$1.2/A1929P *(right, upper)*, and $\alpha_1$1.2/H1926A/H1927A (*right, lower*). (c) Normalized I_{Ba} records from representative oocytes expressing Cav1.2 (wt) and Cav1.2A1929P (*left)* and Normalized I_{Ba} records from representative oocytes expressing Cav1.2 (wt) and Cav1.2H1926A/H1927A (*right*) (d) Steady-state inactivation was recorded in stimulated oocytes according to a multistep protocol of VDI (*inset*). Smooth curves were generated from a single Boltzmann function of wt and the mutated channels as indicated. Values are displayed as mean ± S.E.M (n=10−12). Peak currents were: For HH/AA experiment: $\alpha_1$1.2, −1140±98 nA (n=12); $\alpha_1$1.2/HH/AA, −1560±162 nA (n=14); The A1929P experiment: $\alpha_1$1.2, −398 ± 58 nA (n=8); $\alpha_1$1.2/A1929P, −316±33 (n=21).

Previously we showed that a truncated human $\alpha_1$1.2, in which the CaN binding motif was deleted by a premature stop codon inserted at G1911, led to an increase in VDI (data not shown). To define a specific correlation between CaN-binding site at the human $\alpha_1$1.2 and VDI, we used a single point mutant of $\alpha_1$1.2 (**Fig. 1a, *middle***). *In vitro* studies, carried out in rabbit $\alpha_1$1.2, showed that mutating Ala to Pro (A1959P) at the CaN-site abrogated CaN binding[21,22]. According to these studies, the corresponding human Ala1929 is located within a minimal CaN binding site spanning L1920 and L1935 of the human $\alpha_1$1.2 tail (**Fig. 1b, *upper***).

Whole-cell currents were recorded from oocytes injected with cRNA corresponding either to the human $\alpha_1$1.2/A1929P or the full-length human $\alpha_1$1.2 subunit together with the auxiliary subunits $\alpha 2\delta 1$ and β2b.

Depolarization produced decaying inward barium current (I_{Ba}) in both Cav1.2 and Cav1.2/A1929P (**Fig. 1c, *left***). Superimposed exemplary I_{Ba} traces showed that A1929P mutant was inactivated faster than Cav1.2 (**Fig. 1c, *left***). Quantitatively, the smaller ratio of inward current at the end of a 1,000 ms test pulse relative to the peak current (r_{1000}) was 0.43 ± 0.06 for Cav1.2/A1929P compared to 0.62±0.01 for the wt channel, which indicates faster inactivation of the mutant channel (**Supplementary Table S1 online**).

The steady-state voltage inactivation of A1929P mutant was tested and compared to wt channel (**Fig. 1d, *inset***). The Ca_V1.2/A1929P mutant exhibited virtually complete voltage-dependence of I_{Ba} inactivation, compared to VDI of Cav1.2 (**Fig. 1d, *left*, Table 1**). The Boltzmann curve of the A1929P mutant was shifted to hyperpolarizing potentials, compared to the full-length native Cav1.2 (**Table 1**). A plausible explanation for a stronger VDI is that the A1929P mutation interferes with CaN-binding to the $\alpha_1$1.2 C-tail[21,22], and alleviates an inhibitory effect of CaN on VDI.

To further confirm the CaN binding site a VDI-negative regulatory site, we examined two neighboring vicinal His residues, H1926, H1927, positioned within the minimal CaN binding domain[21,22] for their effect on VDI (**Fig. 1a *lower;* Fig. 1b lower**).

Whole-cell I_{Ba} were recorded from channels co-expressing either wt $\alpha_1$1.2 or $\alpha_1$1.2/HH/AA together with the auxiliary $\alpha_2\delta_1$ and β_{2b}. Superimposed exemplary I_{Ba} traces showed that Cav1.2/HH/AA was inactivated faster than Cav1.2 (**Fig. 1c *right***). Similar to the enhanced inactivation displayed by the A1929P mutant, the smaller ratio of inward current at the end of a 1,000 ms test pulse to the peak current (r_{1000}) of Cav1.2/HH/AA indicated 0.37±0.02 compared to 0.62±0.01 of wt channel, showing faster inactivation than the wt Cav1.2 (**Supplementary Table S1 online**). The Ca_V1.2/HH/AA mutant exhibited virtually complete voltage-dependence of inactivation, compared to the partial VDI of Cav1.2 (**Fig. 1d, *right*; Table 1**). Although the effect of the H1926A/H1927A mutation on CaN binding was not shown through a direct binding, it seemed to up regulate VDI, similar to A1929.

Direct inhibition of CaN increases the extent of voltage inactivation. To confirm that CaN operates as a VDI-regulatory protein, we employed a pharmacological approach, using cyclosporin A (CsA), a potent and selective CaN inhibitor[31]. CsA was used in a concentrations range of 0.01–2 μM, since at a level of 20 μM it increases the probability of channel openings[32].

The I_{Ca} of wt Cav1.2 decayed fast, as shown by the current traces (**Fig. 2a *left***), and by the nearly complete voltage-dependent steady-state inactivation at +10 mV (**Fig. 2b, *left***). The presence of 2 μM CsA did not change the inactivating profile (**Fig. 2a, *left;* Supplementary Table S1 online**) or the extent of I_{Ca} inactivation (**Fig. 2b, *left***). Hence, 2 μM CsA does not affect the wt channel, when it is fully inactivated by the combined action of CDI + VDI.

In the absence of CDI, when Ba^{2+} is the charge carrier, the Cav1.2 currents decayed slowly, driven by the limited VDI mechanism (**Fig. 2b, *right***). The presence of 0.6 μM or 2 μM CsA dramatically increased this partial inactivation of wt Cav1.2 (**Fig. 2b, *right;* Supplementary Table S1 online**), and shifted the Boltzmann curves towards hyperpolarizing voltages (**Fig. 2b, *right;* Table 1**). This shift was not seen in the channel mutants and could be mediated by CsA inhibiting an additional CaN binding motif[21]. Hence, the presence of CsA imposed a full VDI upon the native Cav1.2. In contrast with the considerable effects on inactivation, the activation kinetics of wt channel was only marginally affected by 0.2 or 1 μM CsA (I_{Ca}) (**see Supplementary Fig. S1 online**). Current amplitude was decreased in the presence of 2 μM CsA (I_{Ba}), but there were no significant changes in the time constant of activation, or I/Imax (**see Supplementary Fig. S2 online**).

The A1929P mutation at the CaN-binding site restores inactivation of the Timothy channel. A single missense mutation, G406R in exon 8a of the cardiac L-type calcium channel (*CACNA1C*, Ca_v1.2, $\alpha_1$1.2) was shown to cause the Timothy syndrome (TS), which is as characterized by a prolongation of QT intervals (designated LQT8) due to a significant loss of voltage inactivation of Cav1.2[13,14,33–35].

Since the major effect of the G406R mutation on the TS channel was a loss of VDI, we tested VDI regulation by this well-defined CaN-regulatory site in the TS channel

Initially, the $\alpha_1$1.2/G406R subunit of the Timothy channel was mutated to $\alpha_1$1.2/G406R/A1929P, and the kinetics of inactivation were tested, using voltage-clamped oocytes (Experimental Procedures; **Fig. 3a**).

Representative normalized I_{Ca} or I_{Ba} traces showed faster inactivation of Cav1.2/G406R/A1929P compared to unmodified TS Cav1.2/

Table 1 | Steady-state inactivation parameters of wt Ca_V1.2 and TS channel Ca_V1.2G406R

Charge Carrier	Alpha subunit	Cmax (%)	$V_{1/2}$ (mV)	n	p value
Ca^{2+}	$\alpha_1$1.2	95±3.3	−30.6 ± 2.1	10	
	$\alpha_1$1.2/A1929P	93±3.2	−25.8±3.8	9	
	$\alpha_1$1.2/HH/AA	99±2.6	−30.5±1.6	8	
	$\alpha_1$1.2 /G406R	38±4.3	−30.2 ± 1.5	10	
	$\alpha_1$1.2/G406R + 0.05 μM CsA	76±6.0	−75.7 ± 33.1	8	< 0.005
	$\alpha_1$1.2/G406R/A1929P	71±2.9	−9.9 ± 1.5	8	< 0.005
	$\alpha_1$1.2/G406R/HH/AA	77±4.5	−21.1 ± 2.2	8	< 0.005
Ba^{2+}	$\alpha_1$1.2	58±2.4	1.34 ± 2.4	14	-
	$\alpha_1$1.2/A1929P	91±3.2	−12.1 ± 3.6	8	
	$\alpha_1$1.2/HH/AA	91±3.5	−1.1 ± 3.3	21	< 0.005
	$\alpha_1$1.2/G406R	29±2.2	−30.3 ± 3.5	10–12	-
	$\alpha_1$1.2/G406R/A1929P	61±5.0	−14.1 ± 5.5	13	< 0.005
	$\alpha_1$1.2/G406R/HH/AA	61±1.1	−17.4 ± 9.2	12	< 0.005
	$\alpha_1$1.2/G406R + 0.08 μM CsA	63±4.8	−44.8 ± 5.4	8	< 0.01

$V_{1/2}$, midpoint of steady-state voltage inactivation; Cmax, maximal steady state inactivating current; n=number of oocytes; Student's *t* test (two population) was performed for Cmax.

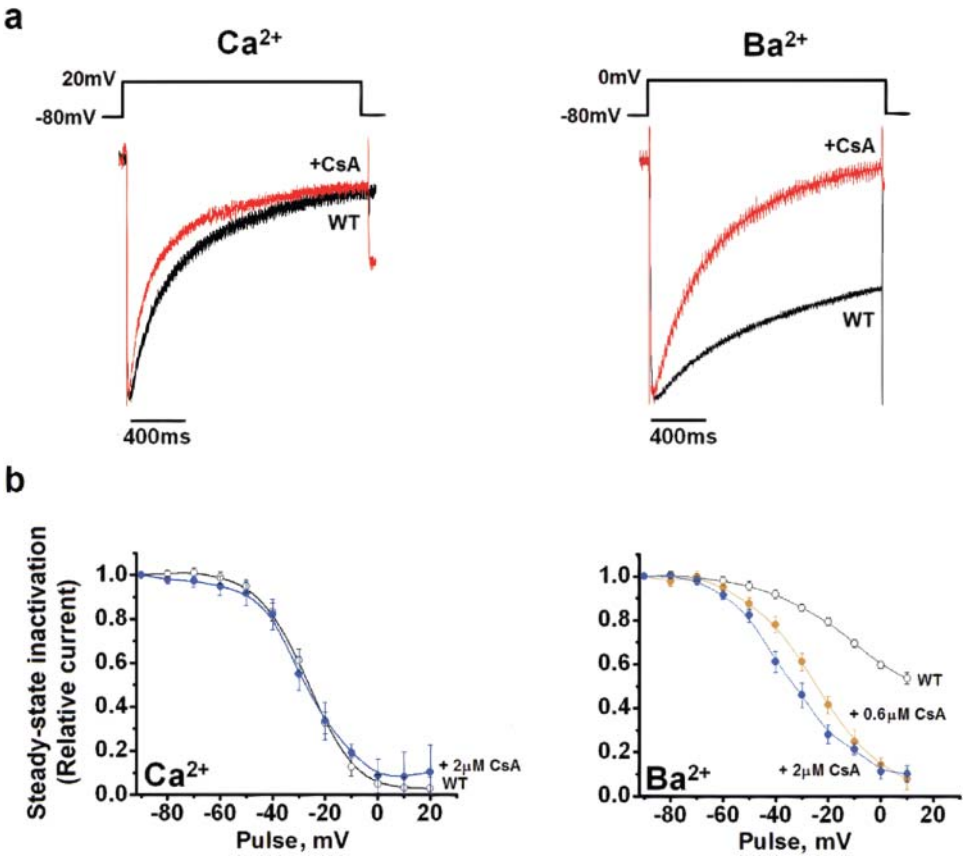

Figure 2 | Cyclosporine A (CsA) increases VDI of Cav1.2. (a) Normalized I_{Ba} and I_{Ca} records from representative oocytes expressing Cav1.2 (wt) in the presence of 2 μM CsA (I_{Ca}) (*left*), or 0.6 and 2 μM of CsA (I_{Ba})(*right*). (b) The voltage-dependence of Cav1.2 inactivation in the presence or absence of CsA (protocol in Fig 1d). Normalized I_{Ca} (*left*) and I_{Ba} (*right*) were fitted to the Boltzmann equation. Values are displayed as mean ±S.E.M (n=10−12). Peak currents for: ICa, $\alpha_1$1.2, −700 ± 57 nA (n=13); $\alpha_1$1.2 +2 μMCsA, −625 ± 76 nA (n=12); IBa, $\alpha_1$1.2, −774 ± 34 nA (n=10) ;$\alpha_1$1.2 +2 μMCsA, −670 ± 69 nA (n=8).

G406R (**Fig. 3b,** (**Supplementary Table S1 online**). Similarly, the steady-state inactivation of both of I_{Ca} and I_{Ba}, displayed elevated Cmax values and a shift in $V_{1/2}$ towards positive potentials (**Fig. 3c, Table 1**). Hence, a single point mutation that abrogates CaN binding to the C-tail of $\alpha_1$1.2 subunit, significantly restored VDI of TS channel.

The HH/AA double mutation at the CaN-binding site of the Timothy channel restores voltage-dependent inactivation. The double mutation HH/AA, inserted in the native human $\alpha_1$1.2 subunit of Cav1.2 channel resulted in a distinctive increase in VDI (see above). To consider the effects of the HH/AA mutation on TS, we mutated the $\alpha_1$1.2/G406R subunit to $\alpha_1$1.2/G406R/HH/AA (**Fig. 4a**). Representative normalized I_{Ca} or I_{Ba} traces showed faster inactivation of Cav1.2/G406R/HH/AA compared to the unmodified Cav1.2/G406R channel (**Fig. 4b**; **Supplementary Table S1 online**). Similarly, the steady-state inactivation of both of I_{Ca} and I_{Ba}, displayed elevated Cmax values and a shift in $V_{1/2}$ towards positive potentials (**Fig. 4c, Table 1**).

Consistent with a previous study[36], the ratio of inactivation rates of inward currents (I_{Ca}/I_{Ba}) based on exemplar normalized traces was significantly different between wt and G406R channels (**see Supplementary Fig. S3 online**). In contrast, there was no significant difference in I_{Ca}/I_{Ba} of wt and the channel mutants, G406R/H1926A/H1927A or G406R/A1929P. This data suggests that in the Timothy channel the motif(s) that regulate CDI proceed independently of VDI regulation by the CaN-binding motif. Since the A1929P and HH/AA mutations in the G406R background, change the I_{ca}/I_{Ba} ratio back to the WT levels, it further suggests that the A1929P and HH/AA mutations also affect the net CDI. A small effect on net CDI was also visible in wt channel mutants (**see Supplementary Fig. S3 online**).

CaN inhibitors increase VDI of Timothy channel. Finally, to further confirm VDI regulation by CaN-binding motif and to establish a prospective strategy for TS treatment, we evaluated the effects of CsA and FK-506 (Tacrolimus) two structurally unrelated CaN inhibitors, on Cav1.2G406R inactivation. The normalized I_{Ca} and I_{Ba} of the Timothy channel showed marked acceleration of inactivation in the presence of 1 μM CsA (**Fig. 5a**). Moreover, the steady-state voltage-dependence of I_{Ca} and I_{Ba} inactivation of the TS channel (**Fig. 5b**) was greater in the presence of CsA. The effects of CsA, at the concentrations as indicated, were accompanied by a strong shift of the Boltzmann curves towards negative voltages (**Fig. 5b, Table 1***).* When plotted against CsA concentration, the Cmax of Cav1.2/G406R at +10 mV displayed an apparent Kd of 27 nM for I_{Ca}, (**Fig. 5c, *upper***) and 37 nM, for I_{Ba} (**Fig. 5c, *lower***). These values correspond to the physiological affinity constant of CsA for CaN[31].

The effects of CsA on maximal inactivation of wt channel (Fig. 2) and TS channel were compared (Fig. 5d). From these results it appears that the CaN binding site is a distinct and specific negative regulator of VDI.

A good control for the convergent effects of CaN using the mutations (A1929P or HH1926-1927AA) or CsA is the lack of additive effect on VDI. In the mutated channels only one of the CaN binding sites is eliminated, while an additional CaN binding site[21], could still bind CaN. Therefore, combining CsA with A1929P or HH/AA

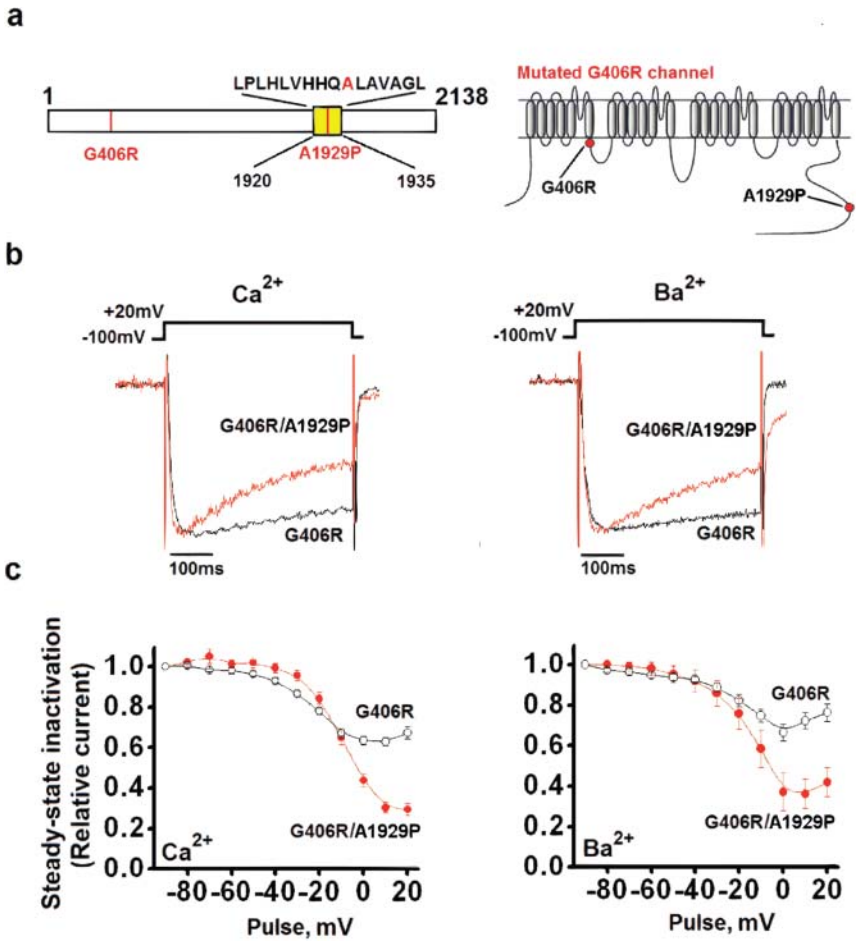

Figure 3 | Single point mutation at CaN binding motif of $\alpha_1$1.2/G406R subunit increases VDI of the Timothy channel. (a) Schematic illustration and location (b) of the G406R Timothy mutation, and the A1929P mutation within the CaN binding motif of the human $\alpha_1$1.2 subunit (c) Normalized I_{Ca} (*left*) and I_{Ba} (*right*) recordings from representative oocytes expressing Cav1.2/G406R and Cav1.2/G406R/A1929P (d) The voltage-dependence of inactivation of Cav1.2G406R and Cav1.2G406R/A1929P in Ca^{2+} (*left*) and Ba^{2+} (*right*). Values are displayed as mean ± S.E.M (n=10−12). Peak currents for ICa, $\alpha_1$1.2/G406R, −493 ± 74 nA (n=13); $\alpha_1$1.2/A1929P −661 ± 115nA (n=8); IBa, $\alpha_1$1.2, −643 ± 57 nA (n=16); $\alpha_1$1.2G406R/A1929P, −1132±18 nA (n=21).

mutants might show an effect mediated either by a second CaN binding site, or by CsA binding at another site.

We showed that 0.2 μM CsA did not affect the rate of inactivation of G406R/A1929P mutant, measured using Ba^{2+} as the charge carrier (**Supplementary Table S1 online**). Also Cmax values, 61±5% compared to 60 ± 7% or V1/2, -14.1±5.5 mV compared to 16.6 ± 6.8 mV, were not affected by the addition of CsA. No additive effect of VDI was observed when 80 μM CsA was applied to the HH/AA/G406R mutant, using Ca^{2+} as the charge carrier (**Supplementary Table S1 online**). Similar to G406R/A1929P and G406R/HH/AA mutants, CsA changed the I_{ca}/I_{Ba} ratio of G406R back to WT level, and appeared to have an effect also on net CDI (**see Supplementary Fig. S3 online**).

Together, these results support the view that CsA acts through inhibiting CaN-binding at the C-tail of $\alpha_1$1.2 to restore the VDI of the channel.

Unlike the strong effects on inactivation, CsA only marginally affected the I_{Ca} current amplitude and activation properties of Cav1.2/G406R (**see Supplementary Fig. S1 online**). CsA displayed a significant increase in the rate of activation of I_{Ba}, slightly affecting I/Imax (**see Supplementary Fig. S2 online**).

Like CsA, FK-506 accelerated I_{Ca} inactivation of the Timothy channel (**Fig. 6a**). It increased current amplitude (**Fig. 6b**) without shifting the I/Imax ratio (**Fig. 6c**) and accelerated activation (**Fig. 6d**). Similar to CsA, with Ca^{2+} as the charge carrier, FK-506 displayed no effect on the steady-state inactivation of the wt channel (**Fig. 6e, *left)*** but increased the steady state of I_{Ba} voltage-inactivation of the TS channel (**Fig. 6e, *right***). The restoration of VDI of the Timothy channel by yet another CaN inhibitor, further confirms that this site is a CaN-specific binding motif that acts as a negative regulatory-motif of Cav1.2.

Discussion

Tandan et al[21] identified a CaN-binding sites on the Ca_V1.2 N- and C- termini. The inhibition of CaN by cyclosporine (CsA) induced an immediate potentiation of Ca_V1.2 currents in neonatal myocytes. This led the authors to suggest that the channel is a CaN substrate where Ca_V1.2 is affected directly by CaN binding rather than through a transcriptional regulation.

The present study identifies the CaN binding-site within the Cav1.2 C-terminus as a regulatory domain of voltage-dependent inactivation (VDI). First, the CaN binding site is demonstrated as a negative regulatory site of normal cardiac channel inactivation, and secondly, the slow VDI, which is a hallmark of Cav1.2 channels bearing the Timothy syndrome (TS) mutation, can be converted into faster wt like VDI by selective inhibition of CaN.

The impact of the distal C terminus on VDI of Ca_V1.2 was tested initially by deleting 227 amino acids from the C terminus of the human $\alpha_1$1.2 subunit (data not shown). The slight increase in VDI

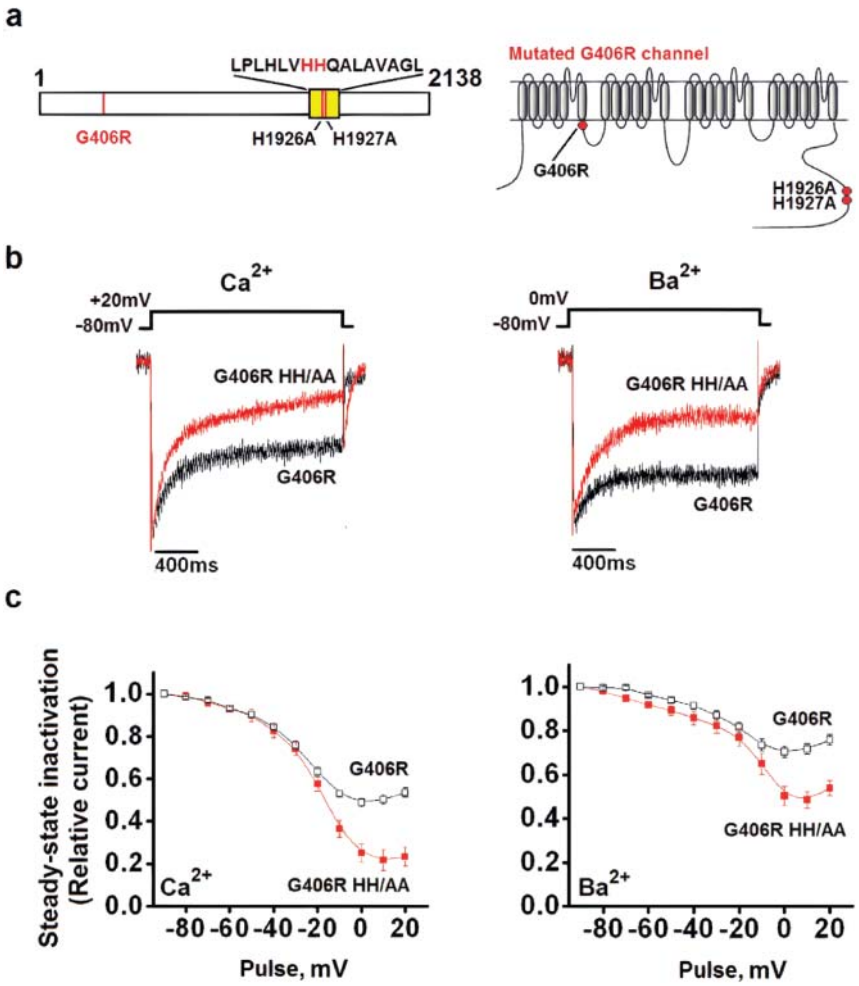

Figure 4 | A mutation within CaN binding motif of TS $\alpha_1$1.2/G406R subunit increases VDI of the Timothy channel. (a) Schematic illustration and location (b) of the Timothy $\alpha_1$1.2G406R subunit and the His1926A, and His1927A mutations within the CaN binding motif of the human $\alpha_1$1.2 subunit (c) Normalized I_{Ca} (*left*) and I_{Ba} (*right*) records from representative oocytes expressing Cav1.2/G406R and Cav1.2/G406R/HH/AA (d) The voltage-dependence of inactivation of Cav1.2G406R and Cav1.2G406R/HH/AA in Ca^{2+} (*left*) and Ba^{2+} (*right*). Values are displayed as mean ± S.E.M (n=10−12). Peak currents for ICa $\alpha_1$1.2/G406R, −493 ± 74 nA (n=13); $\alpha_1$1.2/G406R/HH/AA, −338 ± 52 nA (n=14) For IBa, $\alpha_1$1.2/G406R, −377 ± 61 nA (n=13); $\alpha_1$1.2G406R/HH/AA −518 ± 23 nA (n=10).

observed could result from multiple effects due to the deletion of several regulatory sites, known to reside at the C-terminal of the $\alpha_1$1.2 subunit[1]. Therefore, a more specific target was chosen, which is located within the CaN binding site, previously identified by direct biochemical experiments[21,21]. In these studies mutating Ala to Pro (A1959P) within the minimal CaN binding site L1920-L1935, at the C-tail of $\alpha_1$1.2, abrogated CaN binding. In the present work, the Ca_V1.2/A1929P mutant exhibited virtually complete voltage-dependence of inactivation, compared to the partial VDI of Cav1.2. The importance of this CaN site in regulating VDI was further confirmed by mutating two vicinal histidine residues, which are located within the CaN minimal binding domain at the $\alpha_1$1.2 C-terminus. Although no direct effect of the HH/AA mutation on CaN binding was reported, the Ca_V1.2/HH/AA mutant displayed almost a complete voltage-dependence of inactivation similar to that of the A1929P mutant. Hence, the accelerated rate of inactivation and the increase in the extent of VDI demonstrated by the single and the double mutants, results from interference of CaN binding to the mutated CaN-binding site at the $\alpha_1$1.2 C-tail. Furthermore, it demonstrates that mutating two His residues can prevent CaN function, consistent with it's being part of the minimal binding site for CaN[21]. The stronger VDI establishes the CaN-interaction site as a VDI-negative regulatory motif of Cav1.2. Moreover, like the truncated channel, these results suggest a relief of an inhibitory component, reminiscent of the auto-inhibitory, PKA-dependent regulation of the cardiac channel[37].

The regulation VDI through the CaN binding site was further supported pharmacologically, using CsA. This potent and selective CaN inhibitor significantly increased VDI, suggesting that CsA alleviates an inhibitory constitutive constraint of CaN on VDI. Presumably, an altered interaction of the catalytically-inactive CaN, which remains bound to the CaN-motif at the C-tail[21], interfered with the normal constitutive binding of CaN to the C-tail domain, thereby eliciting complete VDI. The pharmacological approach thus confirmed the results of mutagenesis (A1929P, HH/AA), demonstrating the role of CaN as a negative-regulator of VDI of the cardiac channel. The convergent effects of CsA at the CaN binding-site at $\alpha_1$1.2 C-terminus, further confirms this motif as being a VDI-regulatory site of Cav1.2. This conclusion is congruent with previous findings in mouse ventricular myocytes that CaN inhibition by CaN inhibition by CsA increases the rate of decay of evoked [Ca^{2+}] transients[18].

We then explored whether the CaN regulatory effect could be applied to the slow inactivating Timothy channel[13,14,33–35]. The mechanism by which the G406R mutation decelerates VDI is not yet fully understood[14,38–41,36]. Several reports suggested that G406R generates a

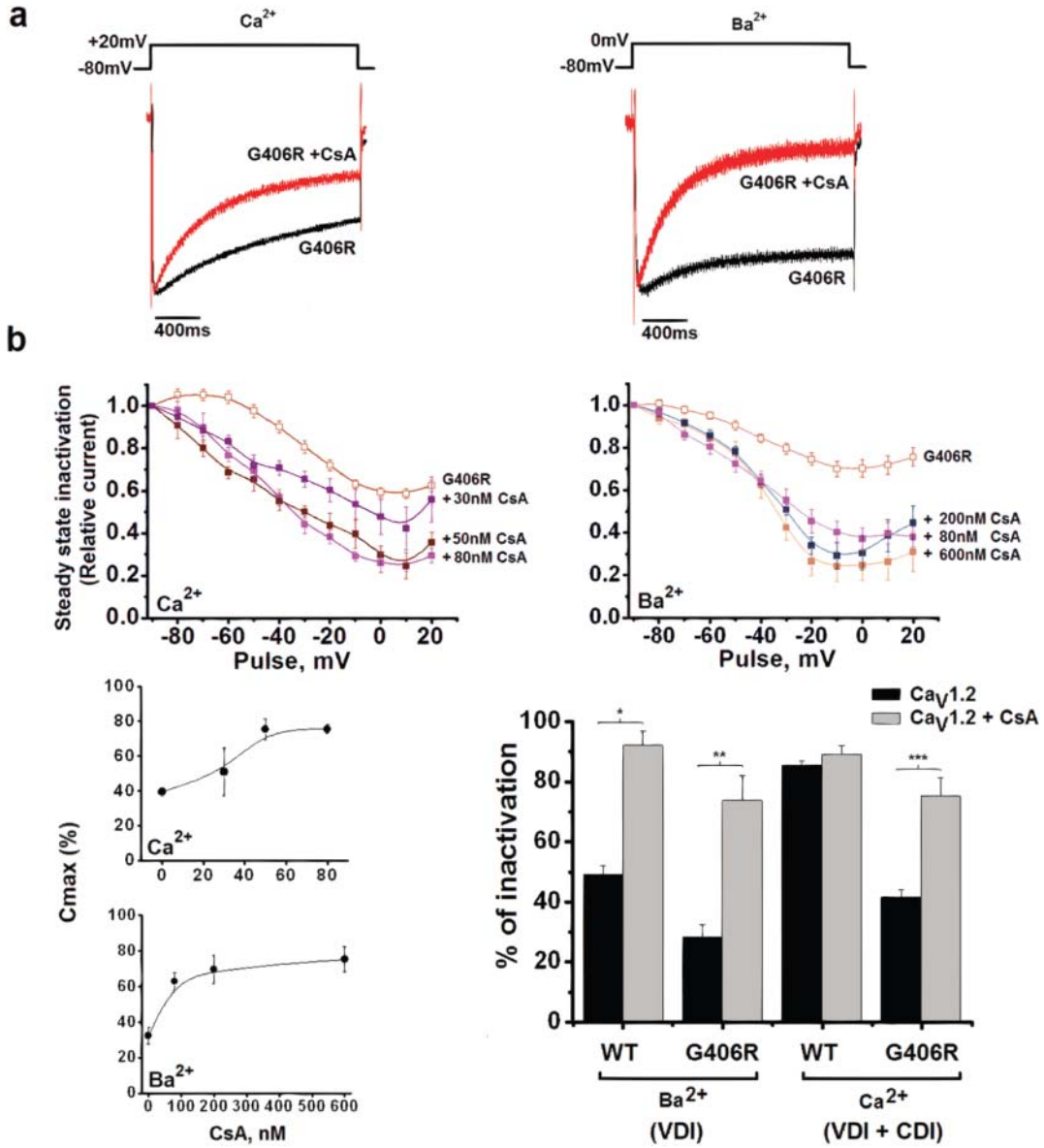

Figure 5 | Cyclosporine A effectively restores VDI of Timothy channel G406R. (a) Normalized I_{Ca} (n=10) (*left*) and I_{Ba} (n=11) (*right*) records from representative oocytes expressing Cav1.2/G406R, in the presence or in the absence of 1 μM CsA. (b) Steady-state inactivation of Cav1.2G406R in the presence of increasing CsA concentrations, as indicated for ICa (*left*) and IBa (*right*). (c) Efficacy of CsA on VDI. Normalized maximal steady-state inactivating I_{Ca} at +10 mV (*left*) and I_{Ba} at 0 mV (*right*) plotted at increasing CsA concentrations. Data displayed as mean ± S.E.M (n=8−12). Peak currents for ICa $\alpha_1$1.2/G406R, −377 ± 40 nA (n=13); $\alpha_1$1.2/G406R + 50 nM CsA, −229 ± 43 nA (n=11); IBa, $\alpha_1$1.2/G406R, −377 ± 61 nA (n=12); $\alpha_1$1.2/G406R + 50 nM CsA, −194 ± 38 nA (n=10).

phosphorylation site for the Ca^{2+}/calmodulin–dependent kinase II, and increases the open probability (P_o) of Ca_V1.2-LQT8 (TS) channels see also[32,39,42]. More recent studies have shown that Ca_V1.2-LQT8 clusters display a higher probability of coordinated openings and closings[41], and a disruption between activation and inactivation of the TS channel[43].

Similar to A1929P and the HH/AA mutated wt channels, both the A1929P and the HH/AA mutated Timothy channels showed a significant increase in the rate and the extent of VDI. The impact of either the single or the double mutations on the VDI of the wt and the Timothy channels is consistent with altered CaN binding to the regulatory motif at the human C-tail of $\alpha_1$1.2. These data support our model, whereby the CaN binding site at $\alpha_1$1.2 serves as a negative-VDI regulatory motif. These results are also consistent with the findings that knockout of the A-kinase anchoring protein AKAP150, an associated scaffolding protein that targets CaN to subcellular sites[19] could restore arrythmogenic mechanisms in LQT8[36].

Furthermore, because the non-TS mutated channel Cav1.2/HH/AA showed a similar increase in VDI (**Fig. 1**), the results favor the interpretation that the distinct CaN-regulatory inactivation determinant at the $\alpha_1$1.2 C-tail acts independently of G406R impairment of VDI.

Finally, using CaN selective inhibitors also showed an increase in VDI of the TS. Similar to the wt channel, CsA was very effective in increasing the rate of inactivation and also FK-506 (Tacrolimus), a structurally unrelated CaN inhibitor also showed acceleration of channel inactivation.

Based on these results, we suggest that CsA or FK-506 have the potential to prevent cardiac associated pathology, and be clinically beneficial for correcting the cardiac malfunction of Timothy patients. These highly efficient CaN inhibitors, which are mainly

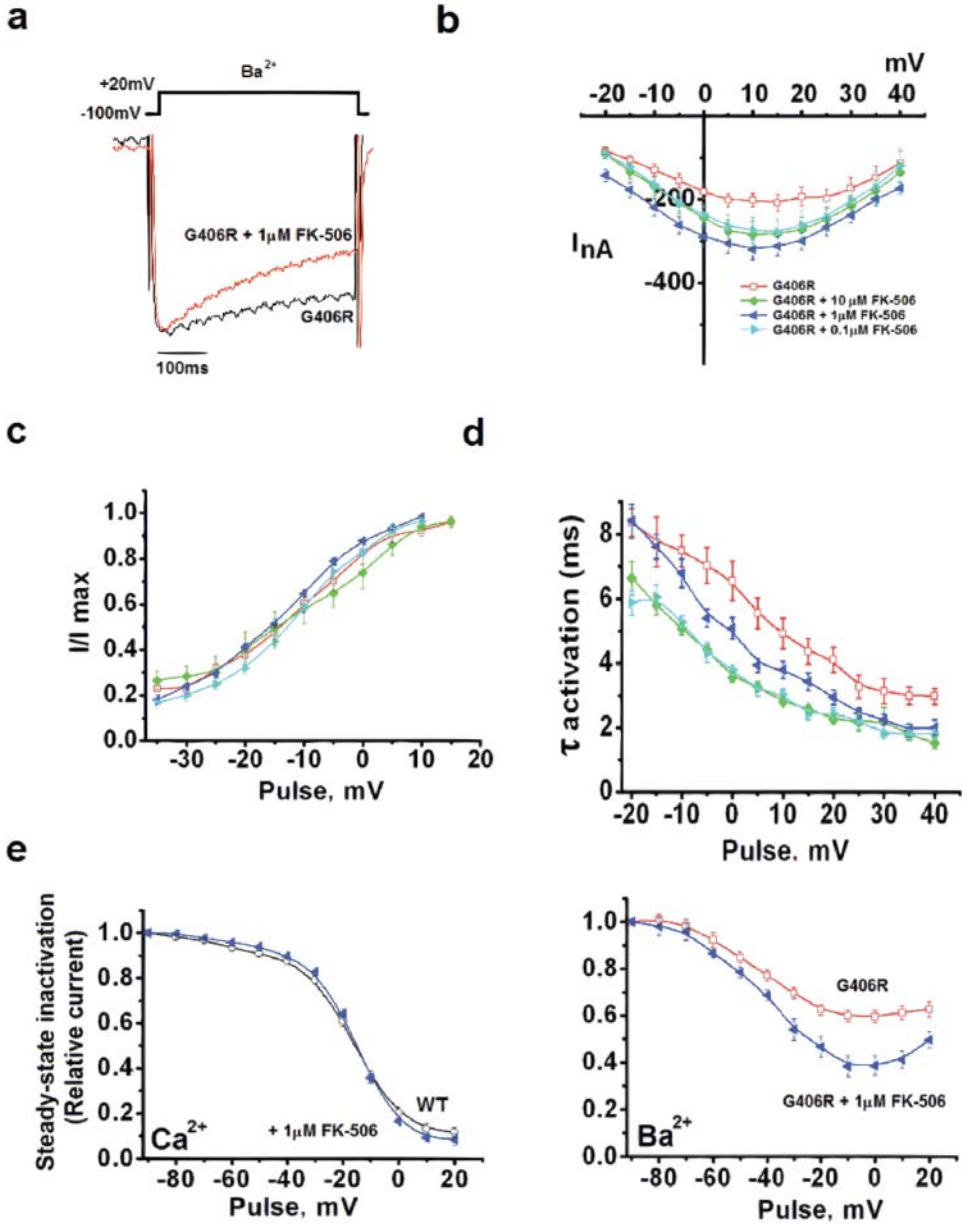

Figure 6 | FK-506 restores Timothy channel inactivation. I_{Ca} was elicited in oocytes expressing $\alpha_1$1.2G406R/$\alpha_2\delta_1/\beta_{2b}$ (Cav1.2G406R) from a holding potential of -80 mV to various test potentials in 5 mV increments, in response to 1200 ms pulse (a) representative I_{Ca} traces elicited in the absence and in the presence of 0.1, 1.0 and 10 μM FK-506 (b) Current–voltage relationship of G406R in the absence and in the presence of FK-506, at the indicated concentrations (c) Peak current amplitudes normalized to maximum current (taken from (b)) shown as I/Imax ratios of inward currents of G406R channel in the presence and in the absence of FK-506 are plotted against test potentials and displayed with a Boltzmann fit (mean ± S.E.M; n = 10–12; more details in supporting online text) (d) The time constant of activation (τact, mean±S.E.M., *n*=10), fitted by a single exponent (e) Steady-state inactivation recorded in stimulated wt (***left***) and G406R channel (***right***) with or without 1 μM CsA, according to a multistep protocol of VDI measurements (Fig. 1C *inset*). Normalized currents were fitted to the Boltzmann equation (Methods).

used as immunosuppressant drugs, increase VDI at low concentrations and hardly alter wt I_{Ca} kinetics.

Thus, CsA can be added to the list of proposed treatments to ameliorate TS related disorders[42,44,45]. Since TS patients often suffer from infections that can be fatal, the use of immunosuppressant's would seem to be contraindicated. Nevertheless, in light of the rather small doses needed to enhance voltage inactivation, the shift in V1/2, the severity of the disease, and the absence of other alternative drugs to treat this syndrome, CaN inhibitors could be of potential clinical use.

In summary, detailed characterization of the kinetics of Cav1.2 and Cav1.2G406R inactivation has identified the CaN-binding site at the C-tail of $\alpha_1$1.2 as a VDI-negative-regulatory motif. The regulation of VDI by CaN, a cytoplasmic Ca^{2+}/calmodulin-dependent protein phosphatase, is consistent with the model of Findlay[4], in which an on/off phosphorylation-dephosphorylation switch is proposed to be responsible for converting a non-inactivating into an inactivating channel. These results also provide a novel rational for "repairing" a non-inactivating Timothy channel by targeting the VDI regulatory motif. The highly selective CaN inhibitors, CsA or FK-506, which effectively increase VDI, offer pharmacologic opportunities as potential candidates for treating Timothy patients.

Methods

Reagents. Cyclosporin A (CsA, M.W 1202.61) was purchased from Novartis. CsA was dissolved in DMSO to a final concentration of 42 mM. FK-506 (Tacrolimus) was purchased from LC Laboratories. FK-506 was dissolved in DMSO to a final

concentration of 10 mM. CsA and FK506 were diluted in the appropriate Ba^{2+} or Ca^{2+} solutions to the desired concentration prior to the experiment.

cDNA Constructs. The full-length human α_1C wt channel (accession # Z34815), the full-length human α_1C G406R, rabbit $\alpha_2\delta_1$ (accession # NM_001082276) and rabbit β_{2b} (accession # X64298) were all cloned in the expression vector pSPORT expression vector. These constructs all were a kind gift from Dr. M. Sanguinetti (University of Utah).

Single mutation. The A1929P mutation was introduced via site-directed mutagenesis of the human $a_1$1.2 or $a_1$1.2/G406R using the following primers: Forward Primer TTG CAT CTG GTT CAT CAT CAG CCA TTG GCA GTG GCA GGC CTG AGC, reverse primer: GCTCAGGCC TGC CAC TGC CAA TGG CTG ATG ATG AAC CAG ATG CAA.

Double mutation. The H1926A, H1927A mutations were introduced via site-directed mutagenesis of the human $\alpha_1$1.2 or $\alpha_1$1.2/G406R using the following primers: Forward Primer-AGA CAG TCC TGC CCT TGC ATC TGG TTG CTG CTC AGG CAT TGG CAG TGG CAG GCC TGA G Reverse Primer-CTC AGG CCT GCC ACT GCC AAT GCC TGA GCA GCA ACC AGA TGC AAG GGC AGG ACT GTC T.

Mutagenesis was performed by PCR of the human template channel using Phusion enzyme (Finnzymes) followed by cleavage with Dpn I and transformation into XL-10 Gold cells (Startagene).

Two-electrode voltage-clamp recordings in *Xenopus* oocytes. Stage V and VI oocytes were surgically removed from female *Xenopus* laevis performed as described[46]. Capped polyA cRNA from linearized cDNA templates encoding wt or mutant human Cav1.2 subunit $\alpha_1$1.2 (5–7 ng), rabbit β_{2b} (2.7 ng), and rabbit $\alpha_2\delta_1$ (5–7 ng) subunits were co-injected into oocytes and whole-cell currents were recorded using the standard two-electrode voltage-clamp configuration as described previously[46]. Briefly Voltage and current 1% agar cushioned electrodes (0.3–0.6-megohm tip resistance) were filled with 3 M KCl. Prior to recording for 15 min, oocytes were injected with 40 nl of solution containing 5 mM HEPES, pH 7.0, and 5 mM of the Ca^{2+} chelator 1,2-bis (2-aminophenoxy) ethane-*N, N, N′, N′*-tetraacetic acid (potassium salt) final concentration (in oocyte).

Activation kinetics. The activation time constants were determined by fitting the raw current data with the equation: $I(t) = I_{max}[1\text{-}\exp(t/\tau_{act})]$, where $I(t)$ indicates the amplitude of current at time t, I_{max} is the maximum amplitude, and τ_{act} is the time constant for activation. Each trace was fitted separately according to Boltzmann, and the averaged values were plotted. Ca_v1.2 activation was fitted to single exponential function. All quantitative results are given as the mean ± S.E. (n = 6–10)[46].

Steady-state inactivation. A multistep protocol was used to determine the steady state of inactivation. A 250 ms control step was applied to +20 mV, followed by a 150 ms repolarization step to -100 mV. Inactivation was tested by applying 4.5 s conditioning pulses from −100 mV to +20 mV in 10 mV increments, followed by a second test pulse of 250 ms to +20 mV.

Voltage-dependence of Ca^{2+} and Ba^{2+} current inactivation was determined with a two-pulse protocol[47]. The fraction of the non-inactivating current was recorded at the end of the pulse at +20 mV, and normalized data were fitted by a single Boltzmann function.

Data acquisition and analyses were performed using pCLAMP9 (Axon Instruments). Currents were filtered at 2 kHz and digitized at 10 kHz. Data were fitted to a Boltzmann function to obtain half point ($V_{1/2}$) and slope factor (k) for the voltage dependence of Ca_V1.2 inactivation. Data are presented as mean ± SEM. The protocol of voltage inactivation is shown in **Fig. 1C *inset***. The fraction of the non-inactivating current was recorded at the end of the pulse at +20 mV, and normalized data were fitted by a single Boltzmann function.

Voltage clamp and data analysis. Inward calcium current (I_{Ca}) and barium current (I_{Ba}) were elicited from a holding potential of −80 mV to various test potentials at 5 mV intervals, by a 1500 ms test pulse.

Channel kinetics was recorded using the standard two-electrode voltage clamp method[48]. Recordings were made in Ba^{2+} solution (in mM): $5Ba(OH)_2$, 50 N-methyl d-glucamine, 1 KOH and 5 HEPES (pH 7.5), titrated to pH 7.5 [$(CH3)_2SO4$] or in Ca^{2+} solution (in mM): $5Ca(OH)_2$, 50 N-methyl d-glucamine, 1 KOH and 5 HEPES (pH 7.5), titrated to pH 7.5 [$(CH3)_2SO4$][48].

Data analysis. *Current inactivation*. The fraction of peak current remaining at the end of a 1,000-ms depolarization (r_{1000}) or at 200 ms (r_{200}), divided by the maximal current was used to quantify the level of inactivation.

Steady state inactivation. curves were fitted by a single Boltzmann distribution with I/Imax=C/{1+exp [$V_{1/2}$−Vm/k]}+(1−C), where C=maximal steady-state inactivating current (Cmax), $V_{1/2}$ =midpoint of inactivation, Vm is the conditioning voltage and k=slope parameter.

The software packages used was pClampfit 9.0 (Axon Instruments, Foster City, CA, USA) and Origin 7.5 (MicroCal).>

1. Catterall, W. A. Structure and regulation of voltage-gated Ca2+ channels. *Annu Rev Cell Dev Biol* **16**, 521-555 (2000).
2. Stotz, S. C. & Zamponi, G. W. Identification of inactivation determinants in the domain IIS6 region of high voltage-activated calcium channels. *J Biol Chem* **276**, 33001-33010 (2001).
3. Budde, T., Meuth, S. & Pape, H. C. Calcium-dependent inactivation of neuronal calcium channels. *Nat Rev Neurosci* **3**, 873-883 (2002).
4. Findlay, I. Physiological modulation of inactivation in L-type Ca2+ channels: one switch. *J Physiol* **554**, 275-283 (2004).
5. Morad, M. & Soldatov, N. Calcium channel inactivation: possible role in signal transduction and Ca2+ signaling. *Cell Calcium* **38**, 223-231 (2005).
6. Cens, T., Rousset, M., Leyris, J. P., Fesquet, P. & Charnet, P. Voltage- and calcium-dependent inactivation in high voltage-gated Ca(2+) channels. *Prog Biophys Mol Biol* **90**, 104-117 (2006).
7. de Leon, M. *et al.* Essential Ca(2+)-binding motif for Ca(2+)-sensitive inactivation of L-type Ca2+ channels. *Science* **270**, 1502-1506 (1995).
8. De Jongh, K. S. *et al.* Specific phosphorylation of a site in the full-length form of the alpha 1 subunit of the cardiac L-type calcium channel by adenosine 3',5'-cyclic monophosphate-dependent protein kinase. *Biochemistry* **35**, 10392-10402 (1996).
9. Soldatov, N. M., Zuhlke, R. D., Bouron, A. & Reuter, H. Molecular structures involved in L-type calcium channel inactivation. Role of the carboxyl-terminal region encoded by exons 40-42 in alpha1C subunit in the kinetics and Ca2+ dependence of inactivation. *J Biol Chem* **272**, 3560-3566 (1997).
10. Peterson, B. Z., DeMaria, C. D., Adelman, J. P. & Yue, D. T. Calmodulin is the Ca2+ sensor for Ca2+ -dependent inactivation of L-type calcium channels. *Neuron* **22**, 549-558 (1999).
11. Zuhlke, R. D. & Reuter, H. Ca2+-sensitive inactivation of L-type Ca2+ channels depends on multiple cytoplasmic amino acid sequences of the alpha1C subunit. *Proc Natl Acad Sci U S A* **95**, 3287-3294 (1998).
12. Hulme, J. T., Yarov-Yarovoy, V., Lin, T. W., Scheuer, T. & Catterall, W. A. Autoinhibitory control of the CaV1.2 channel by its proteolytically processed distal C-terminal domain. *J Physiol* **576**, 87-102 (2006).
13. Splawski, I. *et al.* Ca(V)1.2 calcium channel dysfunction causes a multisystem disorder including arrhythmia and autism. *Cell* **119**, 19-31 (2004).
14. Splawski, I. *et al.* Severe arrhythmia disorder caused by cardiac L-type calcium channel mutations. *Proc Natl Acad Sci U S A* **102**, 8089-8096; discussion 8086-8088 (2005).
15. Molkentin, J. D. *et al.* A calcineurin-dependent transcriptional pathway for cardiac hypertrophy. *Cell* **93**, 215-228 (1998).
16. Rusnak, F. & Mertz, P. Calcineurin: form and function. *Physiol Rev* **80**, 1483-1521 (2000).
17. Bandyopadhyay, A., Shin, D. W., Ahn, J. O. & Kim, D. H. Calcineurin regulates ryanodine receptor/Ca(2+)-release channels in rat heart. *Biochem J* **352 Pt 1**, 61-70 (2000).
18. Santana, L. F., Chase, E. G., Votaw, V. S., Nelson, M. T. & Greven, R. Functional coupling of calcineurin and protein kinase A in mouse ventricular myocytes. *J Physiol* **544**, 57-69 (2002).
19. Oliveria, S. F., Dell'Acqua, M. L. & Sather, W. A. AKAP79/150 anchoring of calcineurin controls neuronal L-type Ca2+ channel activity and nuclear signaling. *Neuron* **55**, 261-275 (2007).
20. Heineke, J. *et al.* Cardiomyocyte GATA4 functions as a stress-responsive regulator of angiogenesis in the murine heart. *J Clin Invest* **117**, 3198-3210 (2007).
21. Tandan, S. *et al.* Physical and functional interaction between calcineurin and the cardiac L-type Ca2+ channel. *Circ Res* **105**, 51-60 (2009).
22. Xu, H. *et al.* Targeting of protein phosphatases PP2A and PP2B to the C-terminus of the L-type calcium channel Ca v1.2. *Biochemistry* **49**, 10298-10307 (2010).
23. Wei, X. *et al.* Modification of Ca2+ channel activity by deletions at the carboxyl terminus of the cardiac alpha 1 subunit. *J Biol Chem* **269**, 1635-1640 (1994).
24. Gao, T. *et al.* cAMP-dependent regulation of cardiac L-type Ca2+ channels requires membrane targeting of PKA and phosphorylation of channel subunits. *Neuron* **19**, 185-196 (1997).
25. Zuhlke, R. D., Pitt, G. S., Deisseroth, K., Tsien, R. W. & Reuter, H. Calmodulin supports both inactivation and facilitation of L-type calcium channels. *Nature* **399**, 159-162 (1999).
26. Ono, K. & Fozzard, H. A. Two phosphatase sites on the Ca2+ channel affecting different kinetic functions. *J Physiol* **470**, 73-84 (1993).
27. Sculptoreanu, A., Rotman, E., Takahashi, M., Scheuer, T. & Catterall, W. A. Voltage-dependent potentiation of the activity of cardiac L-type calcium channel alpha 1 subunits due to phosphorylation by cAMP-dependent protein kinase. *Proc Natl Acad Sci U S A* **90**, 10135-10139 (1993).
28. Davare, M. A., Horne, M. C. & Hell, J. W. Protein phosphatase 2A is associated with class C L-type calcium channels (Cav1.2) and antagonizes channel phosphorylation by cAMP-dependent protein kinase. *J Biol Chem* **275**, 39710-39717 (2000).
29. Mochida, S. & Hunt, T. Calcineurin is required to release Xenopus egg extracts from meiotic M phase. *Nature* **449**, 336-340 (2007).
30. Helekar, S. A., Char, D., Neff, S. & Patrick, J. Prolyl isomerase requirement for the expression of functional homo-oligomeric ligand-gated ion channels. *Neuron* **12**, 179-189 (1994).
31. Swanson, S. K. *et al.* Cyclosporin-mediated inhibition of bovine calcineurin by cyclophilins A and B. *Proc Natl Acad Sci U S A* **89**, 3741-3745 (1992).
32. Erxleben, C. *et al.* Cyclosporin and Timothy syndrome increase mode 2 gating of CaV1.2 calcium channels through aberrant phosphorylation of S6 helices. *Proc Natl Acad Sci U S A* **103**, 3932-3937 (2006).

33. Striessnig, J., Bolz, H. J. & Koschak, A. Channelopathies in Cav1.1, Cav1.3, and Cav1.4 voltage-gated L-type Ca2+ channels. *Pflugers Arch* **460** (2), 361-74 (2010).
34. Liao, P. & Soong, T. W. CaV1.2 channelopathies: from arrhythmias to autism, bipolar disorder, and immunodeficiency. *Pflugers Arch* **460**, 353-359 (2010).
35. Bidaud, I. & Lory, P. Hallmarks of the channelopathies associated with L-type calcium channels: a focus on the Timothy mutations in Ca(v)1.2 channels. *Biochimie* **93**, 2080-2086 (2011).
36. Cheng, E. P. *et al.* Restoration of normal L-type Ca2+ channel function during Timothy syndrome by ablation of an anchoring protein. *Circ Res* **109**, 255-261 (2011).
37. Fuller, M. D., Emrick, M. A., Sadilek, M., Scheuer, T. & Catterall, W. A. Molecular mechanism of calcium channel regulation in the fight-or-flight response. *Sci Signal* **3**, ra70 (2010).
38. Barrett, C. F. & Tsien, R. W. The Timothy syndrome mutation differentially affects voltage- and calcium-dependent inactivation of CaV1.2 L-type calcium channels. *Proc Natl Acad Sci U S A* **105**, 2157-2162 (2008).
39. Thiel, W. H. *et al.* Proarrhythmic defects in Timothy syndrome require calmodulin kinase II. *Circulation* **118**, 2225-2234 (2008).
40. Yazawa, M. *et al.* Using induced pluripotent stem cells to investigate cardiac phenotypes in Timothy syndrome. *Nature* **471**, 230-234 (2010).
41. Navedo, M. F. *et al.* Increased coupled gating of L-type Ca2+ channels during hypertension and Timothy syndrome. *Circ Res* **106**, 748-756 (2010).
42. Yarotskyy, V., Gao, G., Peterson, B. Z. & Elmslie, K. S. The Timothy syndrome mutation of cardiac CaV1.2 (L-type) channels: multiple altered gating mechanisms and pharmacological restoration of inactivation. *J Physiol* **587**, 551-565 (2009).
43. Depil, K. *et al.* Timothy mutation disrupts link between activation and inactivation in CaV1.2. *J Biol Chem* **286**, 31557 (2011).
44. Yarotskyy, V. *et al.* Roscovitine binds to novel L-channel (CaV1.2) sites that separately affect activation and inactivation. *J Biol Chem* **285**, 43-53 (2010).
45. Shah, D. P., Baez-Escudero, J. L., Weisberg, I. L., Beshai, J. F. & Burke, M. C. Ranolazine Safely Decreases Ventricular and Atrial Fibrillation in Timothy Syndrome (LQT8). *Pacing Clin Electrophysiol* **35**, e62-64 (2012).
46. Wiser, O. *et al.* The voltage sensitive Lc-type Ca2+ channel is functionally coupled to the exocytotic machinery. *Proc Natl Acad Sci U S A* **96**, 248-253 (1999).
47. Livneh, A., Cohen, R. & Atlas, D. A novel molecular inactivation determinant of voltage-gated CaV1.2 L-type Ca2+ channel. *Neuroscience* **139**, 1275-1287 (2006).
48. Wiser, O., Bennett, M. K. & Atlas, D. Functional interaction of syntaxin and SNAP-25 with voltage-sensitive L- and N-type Ca2+ channels. *EMBO J* **15**, 4100-4110 (1996).

Acknowledgment

The authors thank H. L. Lauterbach fund and The Betty Feffer Fund for (D.A.) and The Haya and Shlomo Margalit Fund for M.C-K. The authors thank Dr. S. Klein for critically reading the manuscript

Author contribution

YY and MCK performed the experiments, analyzed the data, and prepared the figures. MT prepared the DNA constructs. DA wrote the main manuscript text and prepared figures. All authors reviewed the manuscript.

Additional information

Supplementary information accompanies this paper at http://www.nature.com/scientificreports

Competing financial interests: The authors declare no competing financial interests

How to cite this article: Cohen-Kutner, M., Yahalom, Y., Trus, M. & Atlas, D. Calcineurin Controls Voltage-Dependent-Inactivation (VDI) of the Normal and Timothy Cardiac Channels. *Sci. Rep.* **2**, 366; DOI:10.1038/srep00366 (2012).